JOC Article

Origins of Opposite Syn−Anti Diastereoselectivities in Primary and Secondary Amino Acid-Catalyzed Intermolecular Aldol Reactions Involving Unmodified α-Hydroxyketones

Aiping Fu,* Hongliang Li, Shuping Yuan, Hongzong Si, and Yunbo Duan

Institute for Computational Science and Engineering, Laboratory of New Fiber Materials and Modern Textile, the Growing Base for State Key Laboratory, Qingdao University, Qingdao, Shandong 266071, China

faplhl@eyou.com

Received January 14, 2008

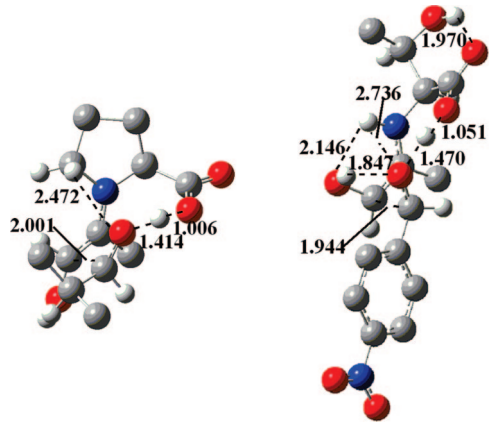

The effects of different amino acid catalysts on the stereoselectivity of the direct intermolecular aldol reactions between α-hydroxyketones and isobutyraldehyde or 4-nitrobenzaldehyde have been studied with the aid of density functional theory methods. The transition states of the crucial C−C bond-forming step with the enamine intermediate addition to the aldehyde for the proline and threonine-catalyzed asymmetric aldol reactions are reported. B3LYP/6-31+G** calculations provide a good explanation for the opposite syn vs anti diastereoselectivity of these two kinds of amino acid catalysts (anti-selectivity for the secondary cyclic amino acids proline, syn-selectivity for the acyclic primary amino acids like threonine). Calculated and observed diastereomeric ratio and enantiomeric excess values are in good agreement.

I. Introduction

Chiral 1,2-diol is a common structural unit that occurs frequently in natural products and biologically active molecules, such as carbohydrates, polyketides, and alkaloids.[1] Recently, significant efforts have been applied toward the development of direct catalytic asymmetric approaches to the construction of this unit based on the addition of unmodified α-hydroxyketones to aldehydes in aldol reactions.[2–4] Although Shibasaki and Trost have provided access to both *syn*- and *anti*-1,2-diols using metal-based catalysis,[2] the development of highly diastereo- and enantioselective organocatalytic approaches remains an important challenge and an appealing area.[3,4] List et. al have reported the first proline (**1**)-catalyzed direct aldol reactions between unmodified hydroxyacetone and various aldehydes to give *anti*-1,2-diols in excellent regio-, diastereo-, and enantioselectivities (eq 1).[3a]

* Corresponding author. Fax: 86-532-85950768.

(1) Nicolaou, K. C.; Snyder, S. A. *Classics in Total Synthesis II*; Wiley-VCH: Weinheim, Germany, 2003, and references therein.

(2) (a) Yoshikawa, N.; Kumagai, N.; Matsunaga, S.; Moll, G.; Ohshima, T.; Suzuki, T.; Shibasaki, M. *J. Am. Chem. Soc.* **2001**, *123*, 2466. (b) Kumagai, N.; Matsunaga, S.; Kinoshita, T.; Harada, S.; Okada, S.; Sakamoto, S.; Yamaguchi, K.; Shibasaki, M. *J. Am. Chem. Soc.* **2003**, *125*, 2169. (c) Trost, B. M.; Ito, H.; Silcoff, E. R. *J. Am. Chem. Soc.* **2001**, *123*, 3367.

(3) (a) Notz, W.; List, B. *J. Am. Chem. Soc.* **2000**, *122*, 7386. (b) Sakthivel, K.; Notz, W.; Bui, T.; Barbas, C. F., III *J. Am. Chem. Soc.* **2001**, *123*, 5260.

(4) (a) Ramasastry, S. S. V.; Zhang, H.; Tanaka, F.; Barbas, C. F., III *J. Am. Chem. Soc.* **2007**, *129*, 288. (b) Ramasastry, S. S. V.; Albertshofer, K.; Utsumi, N.; Tanaka, F.; Barbas, C. F., III *Angew. Chem., Int. Ed.* **2007**, *46*, 5572. (c) Xu, X. Y.; Wang, Y. Z.; Gong, L. Z. *Org. Lett.* **2007**, *9*, 4247.

10.1021/jo800089q CCC: $40.75
Published on Web 06/13/2008

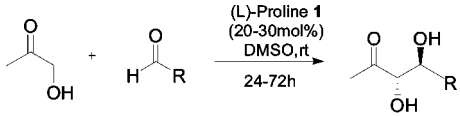

R= i-Pr: 62% yield, anti:syn>20:1, >99%ee;
R= cyclohexane: 60%yield, anti:syn>20:1, >99%ee

Although great advances have been made in the asymmetric direct aldol reactions, highly enantioselective organocatalytic strategies have been limited to antiselectivity. Hence, the new routes of the syn-selective direct aldol reactions have received much research interest. Recently, Barbas' group has developed a simple and efficient strategy to highly enantiomerically enriched *syn*-1,2-diols through direct aldol reactions involving unmodified α-hydroxyketones and 4-nitrobenzaldehyde (eq 2). In these novel asymmetric aldol reactions, primary amine-containing amino acids such as L-threonine (L-Thr, **2**) and O-*t*Bu-L-Thr (**3**) were used as catalysts and the desired *syn*-diols were obtained with high dr (up to 18:1) and ee (up to 98% ee).[4a]

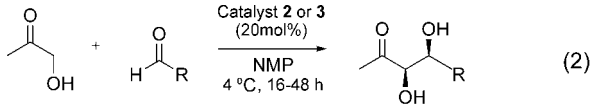

R=p-$NO_2C_6H_4$: for catalyst **2(L-Threonine)**, 75%yield, syn:anti=15:1, 90%ee; for catalyst **3(O-tBu-L-Threonine)**, >95%yield, syn:anti=18:1, 98%ee.

This interesting observation such as different amino acids catalysts leading to opposite syn vs anti diastereoselectivities calls for mechanistic and theoretical investigations. A number of primary and secondary amine-containing amino acids-catalyzed asymmetric direct aldol reactions have previously been studied by density functional theory methods.[5–9] The pioneering theoretical and concomitant experimental studies[10] have established that the reactions proceed via enamine intermediates and the transition states (TSs) for the crucial C−C bond-forming step (nucleophilic addition of the enamine intermediate to an electrophile of aldehyde) showing an arrangement of the reacting atoms that is stabilized by a hydrogen-bonding interaction between the acidic proton of the carboxylic acid moiety in amino acids and the oxygen atom of the electrophile. On the basis of this concept, the diastereo- and enantioselectivity have been successfully rationalized and predicted for the amino acids, especially proline-catalyzed intra- and intermolecular aldol reactions.

To the best of our knowledge, although great efforts have been made to explain the antiselectivity of the direct aldol reactions, there are no other theoretical investigations concerning the syn-selectivity of the primary amino acids-catalyzed aldol reaction between α-hydroxyketones and 4-nitrobenzaldehyde. Therefore, to extend our general understanding of the mechanism and stereoselectivity of the enamine catalytic reactions, the present theoretical study is performed to address the following question: What is the origin of the opposite absolute configuration of products in the secondary amine-containing and primary amine-containing amino acids-catalyzed direct aldol reaction involing α-hydroxyketones as the donor?

II. Computational Methods

All ground state and transition state (TS) geometries were located by using density functional theory (DFT) and the B3LYP hybrid functional.[11,12] The standard 6-31+G** basis sets[13] were employed throughout. All transition state geometries were fully optimized and characterized by frequency analysis. In some cases, the intrinsic reaction coordinate (IRC) pathways were traced to verify the energy profiles connecting the transition structure to the two desired minima of the proposed mechanism. To check the validity of the results at the DFT/DZ computational level, we have reoptimized several important transition states employing the B3LYP/6-311+G** method and the subsequent MP2/6-311+G** single-point energy calculations were carried out on the B3LYP/6-311+G** optimized geometries. Bulk effects of the solvent DMSO for the L-proline-catalyzed and L-threonine-catalyzed processes on the enamine mechanism have been taken into account by means of a dielectric continuum represented by the polarizable conductor calculation model (CPCM), [14] with united-atom Kohn−Sham (UAKS) radii. The single-point continuum calculations were done on the optimized gas phase geometries with a dielectric constant $\varepsilon = 46.7$ for DMSO. All calculations were carried out with the Gaussian 03 program.[15]

III. Results and Discussion

To investigate the secondary amine-containing and primary amine-containing amino acids-catalyzed asymmetric direct aldol reactions involving α-hydroxyketones, we have used L-proline (L-Pro, **1**) and L-threonine (L-Thr, **2**) as the protype catalysts, and eqs 1 and 2 as the model reactions. Scheme 1 shows these catalysts and the notation used for the enamine intermediate and transition states.

Similar to the previous investigation of the aldol reaction, we have focused on the TSs for the enamine attack to the aldehyde.[5–9] This is expected to be the rate-determining step of the reaction because all previous steps leading to enamine are reversible. More importantly, the C−C bond-forming step controls the stereochemistry of the amino acids-catalyzed reactions and thus the ability to study and to understand the observed diastereo- and enantioselectivities. We have considered several stereochemical pathways for this step. First, the enamine intermediate may in principle have a Z or E configuration and the enamine double bond may be oriented syn and anti relative to the carboxylic acid group of the title amino acids (Scheme 1). Second, the different diastereomeric approach modes to the

(5) (a) Bahmanyar, S.; Houk, K. N. *J. Am. Chem. Soc.* **2001**, *123*, 11273. (b) Bahmanyar, S.; Houk, K. N. *J. Am. Chem. Soc.* **2001**, *123*, 12911. (c) Bahmanyar, S.; Houk, K. N.; Martin, H. J.; List, B. *J. Am. Chem. Soc.* **2003**, *125*, 2475.

(6) (a) Allemann, C.; Gordillo, R.; Clemente, F. R.; Cheong, P. H.; Houk, K. N. *Acc. Chem. Res.* **2004**, *37*, 558. (b) Clemente, F. R.; Houk, K. N. *Angew. Chem., Int. Ed.* **2004**, *43*, 5766. (c) Clemente, F. R.; Houk, K. N. *J. Am. Chem. Soc.* **2005**, *127*, 11294. (d) Cheong, P. H.; Houk, K. N.; Warrier, J. S.; Hanessian, S. *Adv. Synth. Catal.* **2004**, *346*, 1111.

(7) Rankin, K. N.; Gauld, J. W.; Boyd, R. J. *J. Phys. Chem. A* **2002**, *106*, 5155.

(8) (a) Arno, M.; Domingo, L. R. *Theor. Chem. Acc.* **2002**, *108*, 232. (b) Arno, M.; Zaragoza, R. J.; Domingo, L. R. *Tetrahedron: Asymmetry* **2005**, *16*, 2764.

(9) Bassan, A.; Zou, W.; Reyes, E.; Himo, F.; Cordova, A. *Angew. Chem., Int. Ed.* **2005**, *44*, 7028.

(10) (a) Hoang, L.; Bahmanyar, S.; Houk, K. N.; List, B. *J. Am. Chem. Soc.* **2003**, *125*, 16. (b) List, B.; Hoang, L.; Martin, H. J. *Proc. Natl. Acad.Sci. U.S.A.* **2004**, *101*, 5839.

(11) (a) Becke, A. D. *J. Chem. Phys.* **1993**, *98*, 1372–1377. (b) Becke, A. D. *J. Chem. Phys.* **1993**, *98*, 5648–5652. (c) Becke, A. D. *Phys. Rev. A* **1988**, *38*, 3098–3100.

(12) Lee, C.; Yang, W.; Parr, R. G. *Phys. Rev. B* **1988**, *37*, 785–789.

(13) (a) Ditchfield, R.; Hehre, W. J.; Pople, J. A. *J. Chem. Phys.* **1971**, *54*, 724. (b) Hehre, W. J.; Ditchfield, R.; Pople, J. A. *J. Chem. Phys.* **1972**, *56*, 2257. (c) Hariharan, P. C.; Pople, J. A. *Theor. Chim. Acta.* **1973**, *28*, 213.

(14) (a) Barone, V.; Cossi, M. *J. Phys. Chem. A.* **1998**, *102*, 1995. (b) Barone, B.; Cossi, M.; Tomasi, J. *J. Comput. Chem.* **1998**, *19*, 404.

(15) Frisch, M. J. *Gaussian03*, Revision D.01; Gaussian, Inc.: Wallingford, CT, 2004.

SCHEME 1

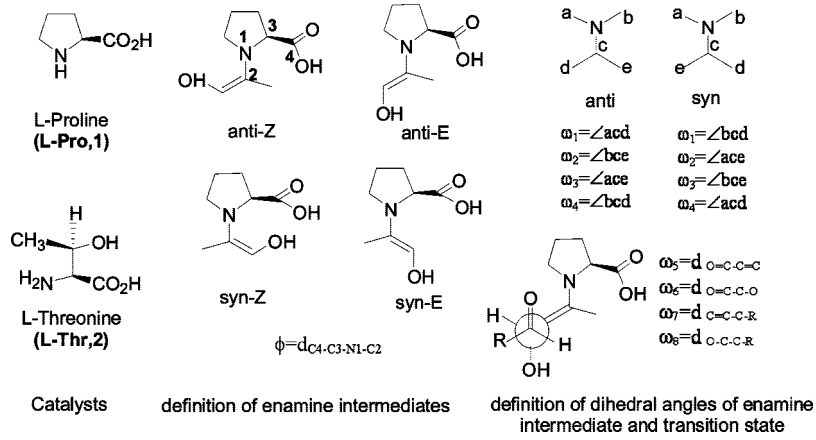

SCHEME 2. Potential Transition States of the Proline-Catalyzed Aldol Reaction between Hydroxyacetone and Aldehydes

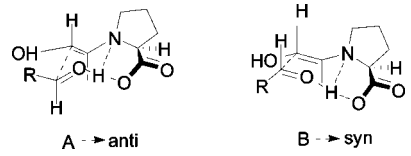

re and *si* faces of enamine and of the carbonyl group of the aldehyde should be considered. Consistent with the previous theoretical studies,[5–9] only transition states that involve hydrogen bonding between the carboxylate and the aldehyde were considered here.

L-Proline-Catalyzed Process. Equation 1 illustrated the antiselectivity of the proline-catalyzed aldol reaction involving unmodified hydroxyacetone performed by List et al.[3a] Excellent diastereo- and enantioselectivity were obtained for the cyclohexanecarboxaldehyde and isobutyraldehyde. The reaction between hydroxyacetone and isobutyraldehyde has been chosen as the model to investigate the stereoselectivities addressed with proline catalyst. In their original work, List et al. have proposed the plausible transition states and the origin of the antiselectivity (Scheme 2). The stereoselectivities of the above reactions have been rationalized with a Zimmerman−Traxler six-membered-ring chairlike model[16] (shown in Scheme 2). The enamine double bond is assumed to possess an (*E*)-configuration and the attack of the *si*-face of the hydroxyacetone (*E*)-enamine to the *re*-face of the aldehyde leads to the major product of *anti*-1,2-diols, while the enamine attack to the *si*-face of aldehyde yields the minor product of *syn*-diols.

Our interests in organocatalysis[17] prompt us to carry out a theoretical investigation of the above hypothesis. We first explored the four isomers of the enamine intermediates formed between proline and α-hydroxyketones (Scheme 1 and Figure S1 in the Supporting Information). The relative energies between different isomers are shown in Table 1 (CPCM values in DMSO are presented in parentheses). Contrary to the hypothesis by List et al., (*Z*)-enamine is a little more stable than (*E*)-enamine with the vinylamine framework distorting greatly to avoid the steric hindrance between the methylene in the pyrrolidine ring and the hydroxyl group (see the dihedral angles listed in Figure S1, Supporting Information). There is only a small energy difference between the two conformers of (*Z*)-enamine, while the *syn*-(*E*)-enamine conformer is much lower in energy than the *anti*-(*E*)-enamine conformer. The inclusion of the solvent effect changes the stabilization order of the four isomers with the *syn*-(*Z*)-enamine being the most stable one. However, the energy difference between (*Z*)- and (*E*)-enamine isomers is small and there is no evidence that one isomer should be greatly preferred over the others.

TABLE 1. Relative Energies[a,b] (kcal/mol) of Different Isomers of Proline and Threonine Enamine of Hydroxyacetone

	anti-Z	*anti-E*	*syn-Z*	*syn-E*
enamine proline	0.0 (1.1)	2.0 (2.7)	0.5 (0.0)	0.2 (0.8)
enamine threonine	0.0 (0.0)	3.1 (2.3)	1.8 (1.2)	3.1 (2.8)

[a] From total energies, including zero-point vibrational energies. [b] CPCM values in DMSO are shown in parentheses.

Eight reactive channels corresponding to four stereoisomers that are syn- and antidiastereomeric pairs of enantiomers for the reaction of the proline enamine of hydroxyacetone and isobutyraldehyde have been considered. Although the aldehyde and enamine may adopt different staggered arrangements about the forming bond, on the basis of the pioneering computational studies,[5–9] only the lowest energy transition states leading to the four products have been illustrated in Figure 1. The notation used for the TSs, for example, "anti" and "E" in "*anti*-(*E*)-*si*-*re*" is consistent with previous conventions, "*si*" denotes as the *si* face of enamine, while "*re*" means the *re* face of aldehyde. The corresponding TSs occurring on the opposite side of the proline ring which lack hydrogen bonding stabilization are not considered. As shown in Figure 1, all the transition structures have common features with the models proposed by Houk's group.[5,6] Among these transition states, the most stable one involving the *re* attack of the *anti*-(*E*)-enamine to aldehyde (**1a**) leads to the (3*S*,4*S*)-enantiomer, which is indeed the major product observed experimentally. The other transition states involving (*E*)-enamine (**1b**−**d**) are at least 5.0 kcal/mol higher in energy than **1a**. Contrary to the hypothesis by the experimental work, the computed TSs involving (*Z*)-enamine should have been considered to rationalize the diastereoselectivity and enantioselectivity. The (3*S*,4*R*)-enantiomer is mainly formed through the transition state **1g** corresponding to the *syn*-(*Z*)-enamine attacking the *si* face of aldehyde. This transition state lies 1.1 kcal/mol higher in energy than the most stable one **1a** in the gas phase. This energy difference increases to 2.1 kcal/mol when the solvent effect is taken into account. Thus the high

(16) Zimmerman, H. F.; Traxler, M. D. *J. Am. Chem. Soc.* **1957**, *79*, 1920.
(17) (a) Fu, A. P.; List, B.; Thiel, W. *J. Org. Chem.* **2006**, *71*, 320. (b) Fu, A. P.; Thiel, W. *J. Mol. Struct. (THEOCHEM)* **2006**, *765*, 45.

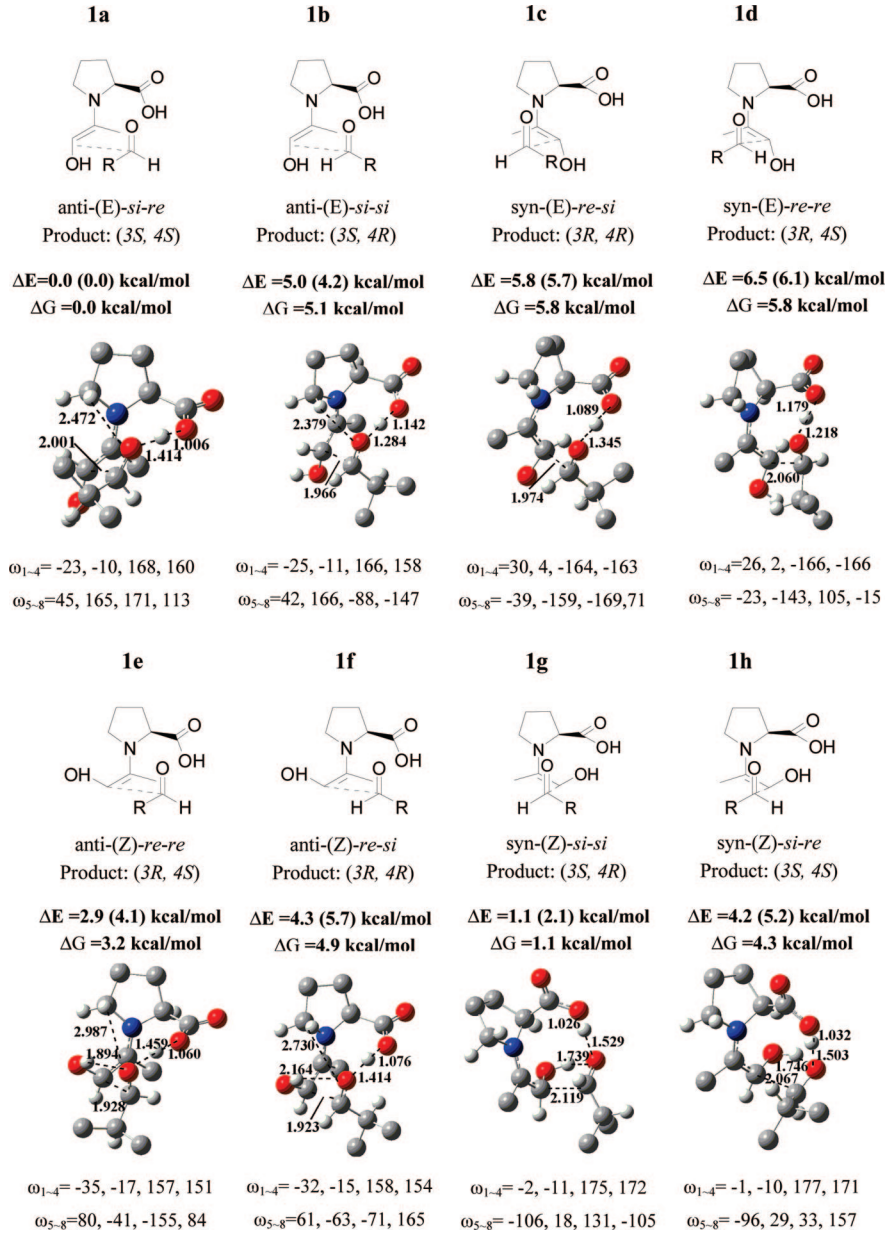

FIGURE 1. Transition structures, relative energies, and relative free enthalpies for the reaction of the proline-enamine of hydroxyacetone with isobutyraldehyde. CPCM values in DMSO are shown in parentheses. For clarity, some of the hydrogen atoms at the periphery are omitted. Different TS arrangements of aldehyde and enamine along the forming C−C bond that generate the four diastereoisomers are shown.

antidiastereoselectivity (dr > 20:1) can be explained. The (3*R*,4*R*)-enantiomer generated from the *si* attack of *anti*-(*Z*)-enamine to aldehyde also requires a higher energy barrier (4.3 kcal/mol), which is in good agreement with the experimental results (>99% ee).

To validate the above results at the B3LYP/6-31+G** computational level, we have reoptimized several important transition states (1a, 1e, and 1g) using the B3LYP/6-311+G** method. Subsequently, the MP2/6-311+G** single-point energy calculations were carried out on the above optimized geometries. The relative energies of those three transition states at different levels of theory are summarized in the Supporting Information (Table S2). As shown in the table, enlarging the basis sets to the triple-ζ quality leads to similar results with those using double-ζ ones. Although the MP2 single-point energy calculations yield the results deviating from those of the DFT method to some extent, they can still give a good description of the diastereoselectivities. Therefore, our results at the DFT/DZ computational level are reliable.

To further verify the reliability of our computational results, the differences in the calculated free activation enthalpies $\Delta\Delta G^{\ddagger}$ (the free enthalpies were derived from the gas phase enthalpies at 298.15 K, using $\Delta\Delta G = \Delta\Delta H - T\Delta\Delta S$, please see Table S3 in the Supporting Information) have been used to predict absolute stereoselectivities such as the associated enantiomeric excess (ee) and diasteromeric ratio (dr) from absolute rate theory, $\ln(k_{anti}/k_{syn}) = \Delta\Delta G^{\ddagger}/RT$. Table 2 lists the corresponding $\Delta\Delta G^{\ddagger}$, ee, and dr values in the gas phase and in DMSO solution, and compares them with the available experimental data.[3a] There is obviously excellent agreement between the predicted and observed stereoselectivities.

TABLE 2. Free Activation Enthalpies $\Delta\Delta G^{\ddagger}$ (kcal/mol), ee, and dr Values versus Experimental Results

	theory (gas phase)				theory (DMSO)[a]				experiment[b]	
catalyst	$\Delta\Delta G_1^{\ddagger}$	ee	$\Delta\Delta G_2^{\ddagger}$	dr	$\Delta\Delta G_1^{\ddagger}$	ee	$\Delta\Delta G_2^{\ddagger}$	dr	ee	dr
proline	4.9	>99%	1.1	6:1	5.7	>99%	2.1	34:1	>99%	>20:1
threonine	4.1	99%	1.7	16:1	2.8	98%	2.2	41:1	90%	15:1

[a] Values for DMSO derive in fact from the electronic energies. [b] Experimental data from refs 3a and 4a, respectively.

Figure 1 provides numerical values for several geometric parameters that are relevant for the relative stability of the TSs. These include the length of the forming C−C bond and the hydrogen bond, and the distance involved in the electrostatic interactions, the dihedral angles ω_{1-4} that are commonly used to measure the deviation of the developing iminium bond from planarity (ideally 0, 0, 180°, and 180°, see Scheme 1), and the dihedral angles ω_{5-8} that represent the different arrangements of aldehyde and enamine along the forming C−C bond (ideally ± 60° and 180° for staggering conformation). Analysis of the geometrical arrangements of the above transition states that lead to the four different diastereoisomers allows us to identify the origin of the stereoselectivity in the reaction. The following factors may contribute to the enantioselectivity and diastereoselectivity. First, as has been pointed out previously,[5,6] the stereoselectivity partially arises from the different degrees to which each diastereomeric transition state satisfies iminium planarity. The more stable TS is always associated with a "more planar" iminum moiety. For example, the distortions from the planar iminium bond in transition state **1e** involving *anti*-(*Z*)-enamine are more pronounced as compared with that of TS **1a** involving *anti*-(E)-enamine. However, there is much less out-of-plane deformation of iminium in transition state **1g** than transition state **1e**. Maybe this considerable distortion of the forming iminium double bond away from planarity in **1e** switched the stabilization order of **1e** and **1g**. The second factor that regulates the stereoselectivity is the different arrangements of aldehyde and enamine along the forming C−C bond. Of course, intramolecular hydrogen bonding and steric repulsion may change the ideal arrangement from the staggering to the more eclipsed ones (ω_{5-8} shown in Scheme 1 and Figure 1). However, transition state **1a** should be preferred over the other ones (**1b**−**h**) due to the more staggering orientation at the reaction center. The third factor arises from the different extent to which each diastereomeric transition state stabilizes the forming alkoxide. On the one hand, as has been pointed out,[5,6] TSs **1a** and **1b** have favorable electrostatic interaction of $^{+\delta}$NCH−O$^{\delta-}$ (distances: 2.37−2.47 Å), which contributes to the lower energy of those TSs. On the other hand, transition states involving the (*Z*)-enamine (**1e**−**f**) are lower in energy than transition states involving (*E*)-enamine (**1b**−**d**), which may be primarily due to the extra hydrogen bonding provided by the OH group of the enamine to the forming alkoxide. The hydrogen bond distances in **1e** (1.894 Å) and **1g** (1.739 Å) are relatively shorter than those in **1f** (2.164 Å) and **1h** (2.067 Å), which can also contribute to the unexpectedly lower energy of TS **1g**. In summary, the interplay between these effects ultimately determines the relative energies of the various transition states and subsequently the stereoselectivity.

Threonine-Catalyzed Process. As shown in eq 2, Barbas et al. have reported the first syn-selective organocatalytic aldol reaction using unmodified hydroxyketone as donor to install a *syn*-1,2-diol functionality in the products.[4a] In their experiments, the primary amine-containing amino acids like L-threonine (**2**) and O-*t*Bu-L-threonine (**3**) were proved to be the remarkably efficient catalysts with excellent stereoselectivities.

The *syn*-aldol studies are based on their original hypothesis (Scheme 3): with pyrrolidine-derived catalysts or secondary amines, (*E*)-enamine A intermediates predominate because of the steric interaction in (*Z*)-enamine B. The antiselectivity of the product can be explained by transition state C because the *si* face of the (*E*)-enamine reacts. With primary amines, (*Z*)-enamine of hydroxyketones E should predominant over (*E*)-enamines F, and when (*Z*)-enamine E reacts with aldehyde in the C−C bond-forming transition state G, *syn*-aldol products should form predominantly.

On the basis of their design considerations, we then performed the density functional theory calculations on the threonine-catalyzed aldol reaction with hydroxyacetone as the donor and 4-nitrobenzaldehyde as the acceptor. The four isomers of the threonine enamine of hydroxyacetone were first explored and the structures and relative energies at the B3LYP/6-31+G** level were also shown in Figure S1 (Supporting Information) and Table 1. Consistent with the hypothesis by Barbas et al., (*Z*)-enamine isomers are more stable than their (*E*)-enamine counterparts. In particular, in the *anti*-(*Z*)-enamine isomer, the extra hydrogen bonding formed between the O atom in the OH group attached to the enamine double bond and the NH group of the amino acid makes it the most stable isomer among them. The inclusion of the solvent effect does not change this trend.

Unlike the secondary cyclic amino acid proline-catalyzed process, proton transfer to the developing alkoxide in the primary amino acid enamine cannot be only from the carboxylic group, but also from the NH group. This may involve two different reaction mechanisms as has been pointed out previously.[6c,9] However, the theoretical investigation[6c,9] indicates that the amino-catalyzed mechanism requires larger activation energies than the corresponding energies of the carboxylic acid-catalyzed enamine mechanism. Hence this alternative mechanism in the primary amino acids-catalyzed aldol reaction can be safely excluded.

Furthermore, contrary to the proline-derived enamine intermediate, acyclic primary amino acid enamine can rotate about the C_α−N bond, and thus *E*- and *Z*-enamines are possible for both *si* and *re* attacks by aldehyde. Therefore more transition state structures must be considered. In the present work, 16 transition state orientations that generate four stereoisomers have been envisioned. More transition states of different arrangement of enamine and aldehyde along the forming C−C bond, which requires much higher activation energies, are not discussed here. These 16 transition states can be divided into two types that differ in the attack on the opposite face of enamine intermediates (type I: 2a−2h; type II: labeled with a prime, 2a′−2h′), which means products generated by transition states 2a′−2h′ are enantiomers of those by TSs 2a−2h correspondingly. In all cases, TSs 2a′−2h′ are much higher in energy

SCHEME 3

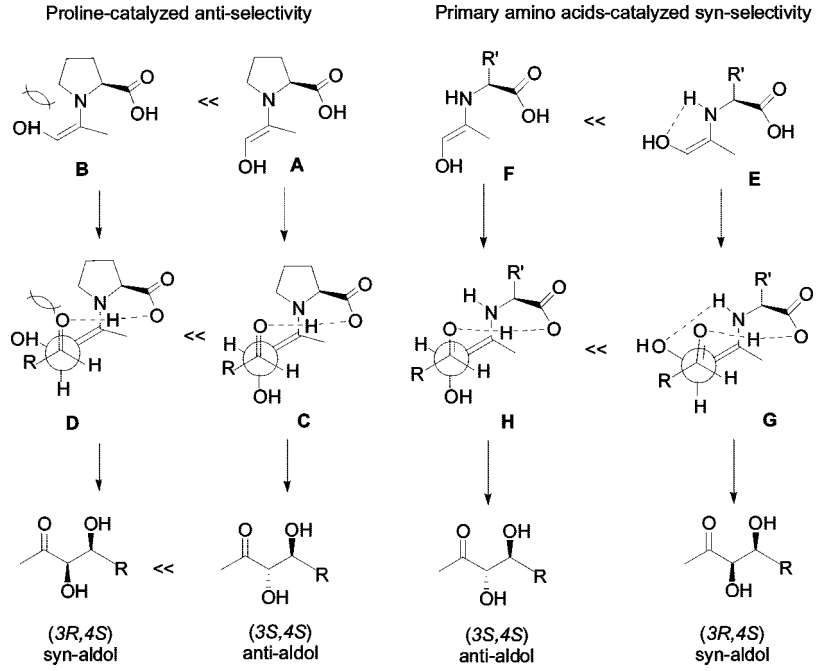

than their counterparts 2a−2h, which indicates that these reactive channels can be excluded in the calculation of the stereoselectivities. However, it should also be noted that in DMSO, transition state 2a′ (2.8 kcal/mol) becomes a bit more stable than 2c (3.4 kcal/mol). The results for the more stable transition states 2a−2h are shown in Figure 2, while the complete list of 16 transition states are given in Supporting Information (Figure S2).

Among the eight lower energy transition states (2a−2h), similar to the results reported for proline catalysis,[5,6] the transition structures with *syn*-enamine (2c, 2d, 2g, 2h) are higher in energy than those with *anti*-enamine (2a, 2b, 2e, 2f). In agreement with the hypothesis by Barbas et al.,[4a] the transition states involving (*Z*)-enamine are more stable than their counterparts involving (*E*)-enamine. The most favored transition state is 2a, which leads to the experimentally observed major product (3*R*,4*S*), the *syn*-1,2-diols. The (3*S*,4*R*)-enantiomer is mainly formed through transition state 2c that lies 4.6 kcal/mol higher in energy, which is consistent with the experimental results (90% ee). The (3*S*,3*S*)-diastereoisomer requires a higher energy barrier (1.8 kcal/mol), thus reasonably explaining the high syn-diastereoselectivity (dr = 15:1).

To verify the calculated results at the DFT/DZ level, the key transition states of 2a, 2b, and 2e have also been reoptimized at the B3LYP/6-311+G** level. The related results are also listed in Table S2 (Supporting Information). It can be concluded that enlarging the basis sets to triple-ζ quality has little effect on the energy difference between those transition states.

The relative stability order of different transition states can also be explained by scrutiny of the geometrical arrangements of the TSs (shown in Figure 2). Here, a new geometric parameter ϕ (shown in Scheme 1)[6c] is introduced to examine the stabilization of the "type I" and "type II" transition states. For type II transition states, the dihedral angel ϕ changes from its ideal value of ∼90° to ∼40°, which is another unfavorable distortion to the stability of the transition states. In fact, this can also be reflected in the distances between the carbonyl acid group and the groups attached on the incipient N=C bond at the reaction center of type I and type II transition states. The so crowded steric disposition of type II TSs makes them greatly destabilized and have no contributions to the diastereoselectivity. Therefore, no further discussion will be made about them.

As has been pointed out in the above proline-catalyzed process, the origin of the stereoselectivity arises from the different degrees to which each diastereomeric transition state satisfies iminium planarity and stabilizes the forming alkoxide, and the different arrangements adopted by enamine and aldehyde along the forming C−C bond. These factors combine to affect the enantioselectivity and diastereoselectivity.

The dihedral angles ω_{1-4} illustrated in Figure 2 indicate that primary amino acids can allow much lower distortion of the enamine systems than with secondary amino acid proline (compare Figure 2 with Figure 1). This is because the conformational flexibility of the acyclic primary amino acids can allow the C_α−N bond to rotate, which subsequently permits the carboxylic moiety to allow the proton transfer more easily with no need of large geometric distortion. However, this is not the case for the proline system due to the conformational restraints imposed by the pyrrolidine ring. Despite the above interplaying factors, when the calculated transition structures for the proline enamine (**1e**) and threonine enamine (**2a**) are compared, TS **2a** also benefits from the extra hydrogen bonding interaction between the O atom in the OH group of enamine and the NH group of amine. Hence, the considerable steric repulsion between the methylene substituent on the proline nitrogen atom and the OH group in (*Z*)-enamine is replaced by the favorable hydrogen bonding interaction in the counterpart of the threonine-catalyzed process, which makes transition state **2a** the most stable one and consequently leads to an inversion in the diastereoselectivity.

The calculated $\Delta\Delta G^{\ddagger}$, ee, and dr values in the gas phase and in DMSO solution of the L-threonine-catalyzed aldol

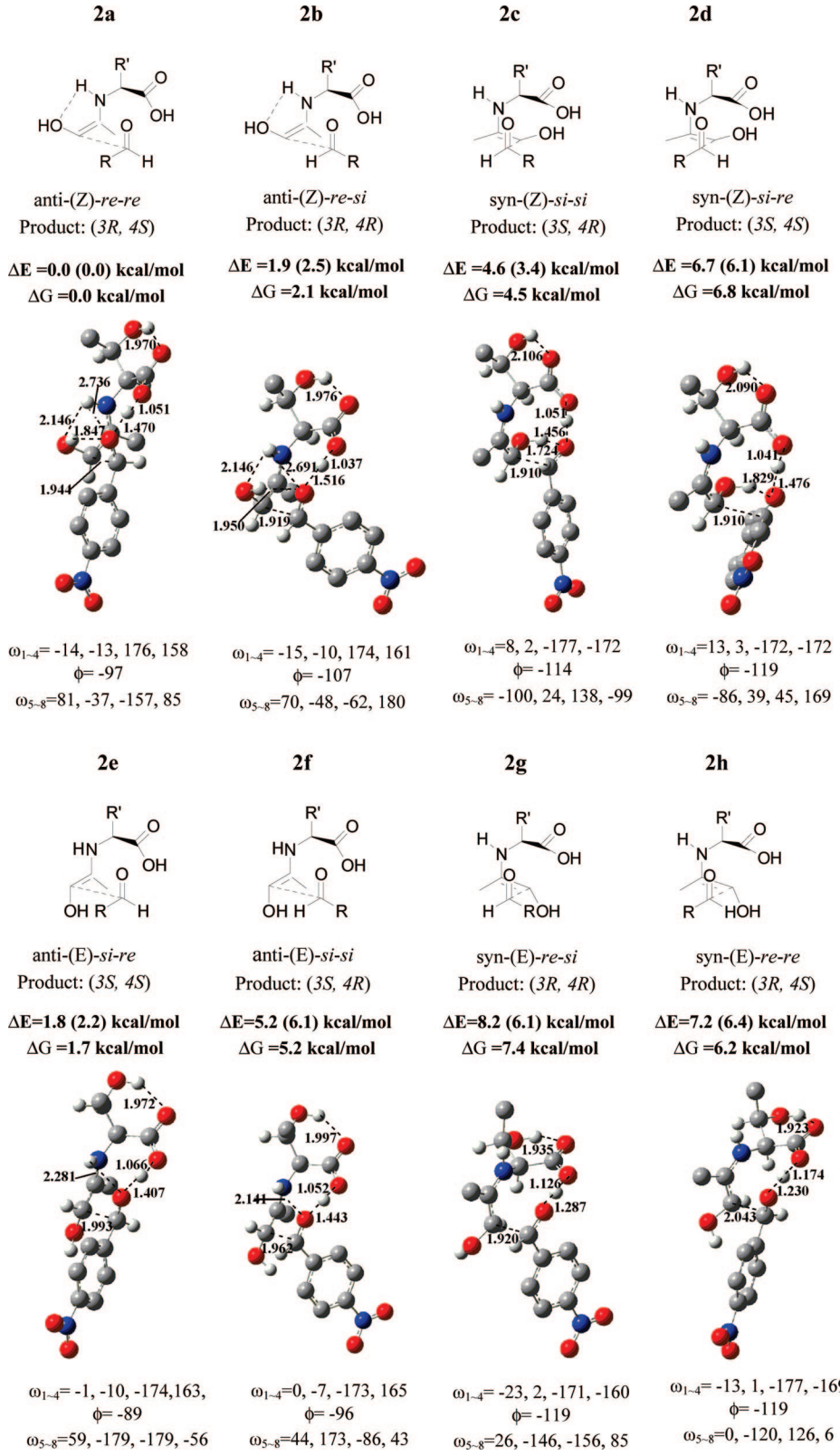

FIGURE 2. Transition structures, relative energies, and relative free enthalpies for the reaction of the threonine-enamine of hydroxyacetone with nitrobenzaldehyde. CPCM values in DMSO are shown in parentheses. For clarity, some of the hydrogen atoms at the periphery are omitted. Different TS arrangements of aldehyde and enamine along the forming C−C bond that generate the four diastereoisomers are shown.

reaction between α-hydroxyketones and 4-nitrobenzaldehyde have also been presented in Table 2 along with the observed experimental results.[4a] Although there is a somewhat overestimation of the experimental ee value, the absolute error can be tolerable and the diastereoselectivity is reproduced satisfactorily.

IV. Conclusions

The transition structures associated with the C−C bond-formation step of the secondary cyclic amino acids proline and acyclic primary amino acids threonine-catalyzed direct aldol reaction involving α-hydroxyketones have been studied by using DFT methods at the B3LYP/6-31+G** computational level. For this stereocontrolling step, all the reactive channels corresponding to the syn and anti arrangement of the enamine double bond relative to the carboxylic group, the two diastereoisomeric approach modes corresponding to the *re* and *si* faces of the carbonyl group of aldehyde, and the *re* and *si* attack of threonine enamine have been studied. Our calculations confirm that the opposite syn vs anti diastereoselectivity found with the proline and threonine arise from the differential steric repulsion between the substituents on the enamine nitrogen (hydrogen in threonine, methylene in proline), with the OH substituent of the *Z*-enamine. In the proline-catalyzed aldol reaction, the steric repulsion with the OH group destabilized the transition states involving (*Z*)-enamine, resulting in the predomination of the TS involving the *anti*-(*E*)-enamine. As a consequence, the *anti*-1,2-diols proved to be the major product. However, in the threonine-catalyzed reactions, the favorable hydrogen bonding interaction between the NH group and the OH substituent instead of the steric hindrance makes the TSs involving *anti*-(Z)-enamine preferred over those involving the *anti*-(*E*)-enamine. This leads to an inversion in the diastereoselectiviy as compared with that of the proline-catalyzed reaction and makes the *syn*-1,2-diols the major product. The calculated diastereomeric ratio and enantiomeric excess are in good agreement with experimental results.

Acknowledgement. This work was supported by the National Natural Science Foundation of China (Nos. 20773071 and 50602028). We also thank the Qingdao University Research Fund for Financial Support (063-06300506).

Supporting Information Available: Cartesian coordinates of all relevant species, total electronic energies and zero point vibrational energies; and the complete ref 15. This material is available free of charge via the Internet at http://pubs.acs.org.

JO800089Q